Acta Mech 220, 217–235 (2011)
DOI 10.1007/s00707-011-0480-4

H. M. Ma · X.-L. Gao · J. N. Reddy

A non-classical Mindlin plate model based on a modified couple stress theory

Received: 31 December 2010 / Accepted: 6 March 2011 / Published online: 1 April 2011

Abstract A non-classical Mindlin plate model is developed using a modified couple stress theory. The equations of motion and boundary conditions are obtained simultaneously through a variational formulation based on Hamilton's principle. The new model contains a material length scale parameter and can capture the size effect, unlike the classical Mindlin plate theory. In addition, the current model considers both stretching and bending of the plate, which differs from the classical Mindlin plate model. It is shown that the newly developed Mindlin plate model recovers the non-classical Timoshenko beam model based on the modified couple stress theory as a special case. Also, the current non-classical plate model reduces to the Mindlin plate model based on classical elasticity when the material length scale parameter is set to be zero. To illustrate the new Mindlin plate model, analytical solutions for the static bending and free vibration problems of a simply supported plate are obtained by directly applying the general forms of the governing equations and boundary conditions of the model. The numerical results show that the deflection and rotations predicted by the new model are smaller than those predicted by the classical Mindlin plate model, while the natural frequency of the plate predicted by the former is higher than that by the latter. It is further seen that the differences between the two sets of predicted values are significantly large when the plate thickness is small, but they are diminishing with increasing plate thickness.

1 Introduction

Microstructure-dependent size effects have been exhibited by many micro- and nano-scale components and devices (e.g., [1,2]). The classical elasticity theory is not capable of predicting such size effects due to the lack of a material length scale parameter.

To overcome this deficiency, several higher-order (non-classical) elasticity theories, which incorporate microstructure-dependent material length scale parameters, have been employed to develop non-classical plate models. Lazopoulos developed a non-classical von Karman plate model [3] based on a simplified strain gradient elasticity theory (SSGET) (e.g., [4–6]) and used it to study the buckling of a long rectangular plate on a rigid foundation. This SSGET, which contains only one material length scale parameter, was also applied in [7,8] to derive non-classical equations of motion for Kirchhoff plates of strain gradient materials. By using a constitutive relation in non-local elasticity suggested in [9], Lu et al. proposed a Kirchhoff plate model and a Mindlin plate model [10] without using a variational formulation. Recently, two new Kirchhoff plate models

H. M. Ma · X.-L. Gao (✉) · J. N. Reddy
Department of Mechanical Engineering, Texas A&M University, College Station, TX 77843-3123, USA
E-mail: xlgao@tamu.edu
Tel.: +1-979-8454835

Present address:
H. M. Ma
Zodiac Aerospace Corporation, Logan, NJ, USA

were developed in [11] and [12] based on a modified couple stress theory [13,14], and another non-classical model for Kirchhoff thin plates was provided in [15] by employing a strain gradient elasticity theory that contains two additional length scale parameters—one related to the bulk strain energy and the other linked to the surface energy.

In addition to these homogenized analyses, Li [16] developed a micromechanics theory for Reissner–Mindlin plates by using a generalized eigen-strain formulation that involves eigen-curvature and eigen-rotation tensors and representing a plate as a Cosserat continuum that includes strain gradient effects, which complemented his work on Love-Kirchhoff plates [17].

The objective of the present paper is to develop a non-classical Mindlin plate model using the modified couple stress theory [13,14] and Hamilton's principle. This modified couple stress theory contains one material length scale parameter and can explain microstructure-dependent size effects. It has been used in developing non-classical models for Bernoulli–Euler beams [18], Timoshenko beams [19], Reddy–Levinson beams [20], and Kirchhoff plates [11,12].

The rest of the paper is organized as follows. In Sect. 2, the modified couple stress theory is first reviewed, which is followed by the evaluations of the first variations of the strain energy, kinetic energy and work by external forces in a Mindlin plate based on the reviewed theory. Hamilton's principle is then applied to derive the governing equations and boundary conditions for the plate, thereby completing the variational formulation of the Mindlin plate model. To illustrate the newly developed plate model, the static bending and free vibration problems of a simply supported plate are analytically solved in Sect. 3. The numerical results quantitatively show the differences between the current (non-classical) and classical Mindlin plate models. The paper concludes in Sect. 4 with a summary.

2 Formulation

According to the modified couple stress theory [13,14,18], the strain energy, U, in an isotropic, linearly elastic material can be written as

$$U = \int_{\Omega} w \mathrm{d}V, \tag{1a}$$

with

$$w = \frac{1}{2}(\boldsymbol{\sigma} : \boldsymbol{\varepsilon} + \boldsymbol{m} : \boldsymbol{\chi}) = \frac{1}{2}\lambda\,(\mathrm{tr}\boldsymbol{\varepsilon})^2 + \mu\left(\boldsymbol{\varepsilon} : \boldsymbol{\varepsilon} + l^2\boldsymbol{\chi} : \boldsymbol{\chi}\right), \tag{1b}$$

where $w = w(\boldsymbol{\varepsilon}, \boldsymbol{\chi})$ is the strain energy density function, Ω is the domain occupied by the material, $\mathrm{d}V$ is the volume element, $\boldsymbol{\sigma}$ is the Cauchy stress tensor, $\boldsymbol{\varepsilon}$ is the strain tensor, $\boldsymbol{m}$ is the deviatoric part of the couple stress tensor, $\boldsymbol{\chi}$ is the symmetric curvature tensor, λ and μ are Lamé's constants in classical elasticity, and l is a material length scale parameter measuring the couple stress effect [18,21]. Note that w in Eq. (1b) contains only the deviatoric part of the couple stress tensor and the symmetric part of the curvature tensor as an energetically conjugated pair, which is different from the strain energy density function in the classical couple stress theory that includes the conjugated pair of the couple stress and the curvature tensor [22,23].

The geometrical equations read

$$\boldsymbol{\varepsilon} = \frac{1}{2}\left[\nabla\boldsymbol{u} + (\nabla\boldsymbol{u})^T\right], \tag{2}$$

$$\boldsymbol{\chi} = \frac{1}{2}\left[\nabla\boldsymbol{\theta} + (\nabla\boldsymbol{\theta})^T\right], \tag{3}$$

where $\boldsymbol{u}$ is the displacement vector, and $\boldsymbol{\theta}$ is the rotation vector defined by

$$\boldsymbol{\theta} = \frac{1}{2}\mathrm{curl}\,\boldsymbol{u}. \tag{4}$$

The constitutive equations are given by

$$\boldsymbol{\sigma} = \lambda\mathrm{tr}(\boldsymbol{\varepsilon})\mathbf{I} + 2\mu\boldsymbol{\varepsilon}, \tag{5}$$

$$\boldsymbol{m} = 2l^2\mu\boldsymbol{\chi}, \tag{6}$$

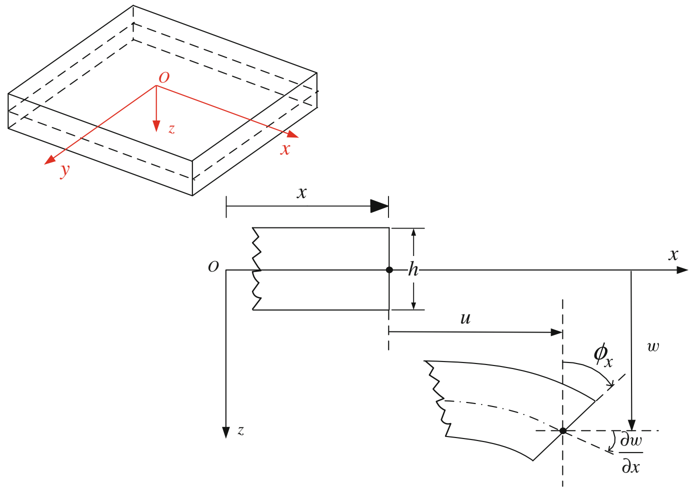

Fig. 1 Plate configuration and coordinate system

where the Lamé constants λ and μ are related to Young's modulus E and Poisson's ratio ν by (e.g., [24]):

$$\lambda = \frac{E\nu}{(1+\nu)(1-2\nu)}, \quad \mu = \frac{E}{2(1+\nu)}. \tag{7}$$

Using Eq. (7) in Eq. (1b) gives w in the following quadratic form:

$$w = \frac{E}{2(1+\nu)}\left[\frac{\nu}{1-2\nu}(\mathrm{tr}\boldsymbol{\varepsilon})^2 + \boldsymbol{\varepsilon} : \boldsymbol{\varepsilon} + l^2 \boldsymbol{\chi} : \boldsymbol{\chi}\right]. \tag{8}$$

It can be shown that the necessary and sufficient conditions for w in Eq. (8) to be positive definite are

$$E > 0, \tag{9a}$$
$$-1 < \nu < 0.5, \tag{9b}$$
$$l^2 > 0. \tag{9c}$$

Note that the first two constraints on Young's modulus E and Poisson's ratio ν in Eqs. (9a, 9b) are necessary and sufficient for the positive definiteness of the strain energy density function in classical elasticity (i.e., the first two terms in Eq. (8)) (e.g., [25,26]), while the third constraint on the new material length scale parameter l in Eq. (9c) ensures that the third term in Eq. (8) (accounting for the couple stress effect) is positive definite. The positive definiteness of the strain energy function is required for the uniqueness of the solution to a boundary value problem in elasticity (e.g., [26]).

It should be mentioned that the conditions listed in Eqs. (9a–9c) for the positive definiteness of the strain energy (density) function in the modified couple stress theory (with one additional material constant l) are only a subset of those in the classical couple stress theory (containing two additional material constants) and are easier to satisfy. In fact, Eq. (9c) is automatically satisfied by all nonzero real values of the material length scale parameter l. The specific value of l for a given material can be determined from torsion tests of slender cylinders [27] or bending tests of thin beams [1]. For polymeric materials containing polymer chains with finite stiffness, l is directly related to the effective Frank constant, which is a microstructural parameter depending on the chain stiffness, the strength of chain interactions, and the cross-link density [28].

Consider a plate of uniform thickness h. By using the Cartesian coordinate system (x, y, z) shown in Fig. 1, where the xy-plane is coincident with the geometrical mid-plane of the undeformed plate, the displacement field in a Mindlin plate can be expressed as (e.g., [29,30])

$$u_1(x, y, z, t) = u(x, y, t) - z\phi_x(x, y, t), \quad u_2(x, y, z, t) = v(x, y, t) - z\phi_y(x, y, t),$$
$$u_3(x, y, z, t) = w(x, y, t), \tag{10}$$

where u_1, u_2 and u_3 are, respectively, the x-, y- and z-components of the displacement vector $\boldsymbol{u}$ of a point (x, y, z) in the plate at time t, u, v and w are, respectively, the components of the displacement vector of the corresponding point $(x, y, 0)$ on the plate mid-plane at time t, and ϕ_x and ϕ_y are, respectively, the rotation angles of a transverse normal about the y-axis and x-axis (see Fig. 1).

From Eqs. (2) and (10), it follows that

$$\begin{aligned} &\varepsilon_{xx} = u_{,x} - z\phi_{x,x}, \quad \varepsilon_{yy} = v_{,y} - z\phi_{y,y}, \quad \varepsilon_{xy} = \frac{1}{2}\left(u_{,y} - z\phi_{x,y} + v_{,x} - z\phi_{y,x}\right), \\ &\varepsilon_{zz} = 0, \quad \varepsilon_{xz} = \frac{1}{2}(w_{,x} - \phi_x), \quad \varepsilon_{yz} = \frac{1}{2}(w_{,y} - \phi_y), \end{aligned} \tag{11}$$

where a comma followed by a subscript denotes differentiation with respect to the subscript (e.g., $u_{,x} = \partial u/\partial x$).

Substituting Eq. (10) into Eq. (4) gives

$$\theta_1 = \frac{1}{2}(w_{,y} + \phi_y), \quad \theta_2 = -\frac{1}{2}(w_{,x} + \phi_x), \quad \theta_3 = \frac{1}{2}\left(v_{,x} - z\phi_{y,x} - u_{,y} + z\phi_{x,y}\right). \tag{12}$$

Using Eq. (12) in Eq. (3) then leads to

$$\begin{aligned} &\chi_{xx} = \frac{1}{2}(w_{,xy} + \phi_{y,x}), \quad \chi_{yy} = -\frac{1}{2}(w_{,xy} + \phi_{x,y}), \quad \chi_{zz} = \frac{1}{2}(-\phi_{y,x} + \phi_{x,y}), \\ &\chi_{xy} = \frac{1}{4}(w_{,yy} + \phi_{y,y} - w_{,xx} - \phi_{x,x}), \quad \chi_{xz} = \frac{1}{4}\left(v_{,xx} - z\phi_{y,xx} - u_{,xy} + z\phi_{x,xy}\right), \\ &\chi_{yz} = \frac{1}{4}\left(v_{,xy} - z\phi_{y,xy} - u_{,yy} + z\phi_{x,yy}\right). \end{aligned} \tag{13}$$

From Eqs. (1a, 1b), the first variation of the total strain energy in the plate on the time interval $[0, T]$ is

$$\delta \int_0^T U \mathrm{d}t = \int_0^T \int_\Omega \sigma_{ij} \delta\varepsilon_{ij} \mathrm{d}V \mathrm{d}t + \int_0^T \int_\Omega m_{ij} \delta\chi_{ij} \mathrm{d}V \mathrm{d}t, \tag{14}$$

where Ω is the region occupied by the plate.

Note that the volume integral of a sufficiently smooth function $F(x, y, z, t)$ over the region Ω can be expressed as

$$\int_\Omega F(x, y, z, t)\mathrm{d}V = \int_R \int_{-h/2}^{h/2} F(x, y, z, t)\mathrm{d}z\mathrm{d}A, \tag{15}$$

where h is the (uniform) plate thickness, and R is the (arbitrary) area occupied by the mid-plane of the plate.

By using Eqs. (11) and (15), the first integral on the right-hand side of Eq. (14) can be determined as, with the help of Green's theorem,

$$\begin{aligned} &\int_0^T \int_\Omega \sigma_{ij} \delta\varepsilon_{ij} \mathrm{d}V \mathrm{d}t \\ &= \int_0^T \int_R \big[-(N_{xx,x} + N_{xy,y})\delta u - (N_{yy,y} + N_{xy,x})\delta v - (N_{xz,x} + N_{yz,y})\delta w \\ &\quad + (M_{xx,x} + M_{xy,y} - N_{xz})\delta\phi_x + (M_{yy,y} + M_{xy,x} - N_{yz})\delta\phi_y\big] \mathrm{d}A\mathrm{d}t \\ &\quad + \int_0^T \int_{\partial R} \big[(N_{xx}n_x + N_{xy}n_y)\delta u + (N_{yy}n_y + N_{xy}n_x)\delta v + (N_{xz}n_x + N_{yz}n_y)\delta w \\ &\quad - (M_{xx}n_x + M_{xy}n_y)\delta\phi_x - (M_{yy}n_y + M_{xy}n_x)\delta\phi_y\big] \mathrm{d}s\mathrm{d}t, \end{aligned} \tag{16}$$

where ∂R is the boundary curve enclosing the area R, ds is the differential element of arc length along ∂R, and

$$N_{xx} \equiv \int_{-h/2}^{h/2} \sigma_{xx}\mathrm{d}z, \tag{17a}$$

$$N_{yy} \equiv \int_{-h/2}^{h/2} \sigma_{yy}\mathrm{d}z, \tag{17b}$$

$$N_{xz} \equiv \int_{-h/2}^{h/2} \sigma_{xz}\mathrm{d}z, \tag{17c}$$

$$N_{yz} \equiv \int_{-h/2}^{h/2} \sigma_{yz}\mathrm{d}z, \tag{17d}$$

$$N_{xy} \equiv \int_{-h/2}^{h/2} \sigma_{xy}\mathrm{d}z, \tag{17e}$$

$$M_{xx} \equiv \int_{-h/2}^{h/2} \sigma_{xx}z\mathrm{d}z, \tag{17f}$$

$$M_{yy} \equiv \int_{-h/2}^{h/2} \sigma_{yy}z\mathrm{d}z, \tag{17g}$$

$$M_{xy} \equiv \int_{-h/2}^{h/2} \sigma_{xy}z\mathrm{d}z \tag{17h}$$

are the stress resultants through the plate thickness.

Using Eqs. (13) and (15) gives the second integral on the right-hand side of Eq. (14) as, with the help of Green's theorem,

$$\begin{aligned}
&\int_0^T \int_\Omega m_{ij}\delta\chi_{ij}\mathrm{d}V\mathrm{d}t \\
&= \frac{1}{2}\int_0^T \int_R [-(Y_{xz,xy} + Y_{yz,yy})\delta u + (Y_{xz,xx} + Y_{yz,xy})\delta v + (Y_{xx,xy} - Y_{yy,xy} + Y_{xy,yy} - Y_{xy,xx})\delta w \\
&\quad +(H_{yz,yy} + H_{xz,xy} - Y_{zz,y} + Y_{yy,y} + Y_{xy,x})\delta\phi_x + (Y_{zz,x} - H_{xz,xx} - H_{yz,xy} - Y_{xx,x} - Y_{xy,y})\delta\phi_y]\mathrm{d}A\mathrm{d}t \\
&\quad +\frac{1}{2}\int_0^T \int_{\partial R} \left\{\left(\frac{1}{2}Y_{xz,x}n_y + \frac{1}{2}Y_{xz,y}n_x + Y_{yz,y}n_y\right)\delta u - \left(Y_{xz,x}n_x + \frac{1}{2}Y_{yz,x}n_y + \frac{1}{2}Y_{yz,y}n_x\right)\delta v \right. \\
&\quad +\left[-\frac{1}{2}(Y_{xx} - Y_{yy})_{,x}n_y - \frac{1}{2}(Y_{xx} - Y_{yy})_{,y}n_x - Y_{xy,y}n_y + Y_{xy,x}n_x\right]\delta w \\
&\quad +\left(Y_{zz}n_y - Y_{yy}n_y - Y_{xy}n_x - \frac{1}{2}H_{xz,x}n_y - \frac{1}{2}H_{xz,y}n_x - H_{yz,y}n_y\right)\delta\phi_x
\end{aligned}$$

$$
\begin{aligned}
&+\left(-Y_{zz}n_x + Y_{xx}n_x + Y_{xy}n_y + H_{xz,x}n_x + \frac{1}{2}H_{yz,x}n_y + \frac{1}{2}H_{yz,y}n_x\right)\delta\phi_y \\
&-\frac{1}{2}Y_{xz}n_y\delta u_{,x} - \left(\frac{1}{2}Y_{xz}n_x + Y_{yz}n_y\right)\delta u_{,y} + \left(\frac{1}{2}Y_{yz}n_y + Y_{xz}n_x\right)\delta v_{,x} + \frac{1}{2}Y_{yz}n_x\delta v_{,y} \\
&+\left[\frac{1}{2}(Y_{xx} - Y_{yy})n_y - Y_{xy}n_x\right]\delta w_{,x} + \left[\frac{1}{2}(Y_{xx} - Y_{yy})n_x + Y_{xy}n_y\right]\delta w_{,y} + \frac{1}{2}H_{xz}n_y\delta\phi_{x,x} \\
&+\left(\frac{1}{2}H_{xz}n_x + H_{yz}n_y\right)\delta\phi_{x,y} - \left(H_{xz}n_x + \frac{1}{2}H_{yz}n_y\right)\delta\phi_{y,x} - \frac{1}{2}H_{yz}n_x\delta\phi_{y,y}\Bigg\}\,\mathrm{d}s\mathrm{d}t,
\end{aligned}
\tag{18}
$$

where

$$
\begin{aligned}
&Y_{xx} \equiv \int_{-h/2}^{h/2} m_{xx}\mathrm{d}z, \quad Y_{yy} \equiv \int_{-h/2}^{h/2} m_{yy}\mathrm{d}z, \quad Y_{zz} \equiv \int_{-h/2}^{h/2} m_{zz}\mathrm{d}z, \quad Y_{xy} \equiv \int_{-h/2}^{h/2} m_{xy}\mathrm{d}z, \\
&Y_{xz} \equiv \int_{-h/2}^{h/2} m_{xz}\mathrm{d}z, \quad Y_{yz} \equiv \int_{-h/2}^{h/2} m_{yz}\mathrm{d}z, \quad H_{xz} \equiv \int_{-h/2}^{h/2} m_{xz}z\mathrm{d}z, \quad H_{yz} \equiv \int_{-h/2}^{h/2} m_{yz}z\mathrm{d}z
\end{aligned}
\tag{19}
$$

are the couple stress resultants through the plate thickness.

The kinetic energy of the plate can be expressed as (e.g., [19,20])

$$
K = \frac{1}{2}\int_{\Omega} \rho[(\dot{u}_1)^2 + (\dot{u}_2)^2 + (\dot{u}_3)^2]\mathrm{d}V, \tag{20}
$$

where ρ is the mass density of the plate material. In Eq. (20) and throughout this paper, the overhead "·" and "··" denote, respectively, the first and second time derivatives (e.g., $\dot{u}_1 = \partial u_1/\partial t,\ \ddot{u}_1 = \partial^2 u_1/\partial t^2$).

From Eqs. (10), (15) and (20), the first variation of the kinetic energy, on the time interval $[0, T]$, is determined to be

$$
\delta\int_0^T K\mathrm{d}t = -\int_0^T\int_R (m_0\ddot{u}\delta u + m_0\ddot{v}\delta v + m_0\ddot{w}\delta w + m_2\ddot{\phi}_x\delta\phi_x + m_2\ddot{\phi}_y\delta\phi_y)\mathrm{d}A\mathrm{d}t, \tag{21}
$$

where

$$
m_0 \equiv \rho h, \quad m_2 \equiv \frac{\rho h^3}{12}. \tag{22}
$$

In reaching Eq. (21), it has been assumed that the initial ($t = 0$) and final ($t = T$) configurations of the plate are prescribed so that the virtual displacements vanish at $t = 0$ and $t = T$. In addition, ρ is taken to be constant along the plate thickness and over the time interval $[0, T]$ such that $\dot{m}_0 = 0,\ \ \dot{m}_2 = 0$.

From the general expression of the work done by external forces in the modified couple stress theory (e.g., [14,18]), the virtual work by the forces applied on the plate on the time interval $[0, T]$ can be shown to be

$$
\begin{aligned}
\delta\int_0^T W\mathrm{d}t = &\int_0^T\int_R \Bigg\{ f_x\delta u + f_y\delta v + f_z\delta w + \frac{1}{2}\big[c_x\delta(w_{,y} + \phi_y) - c_y\delta(w_{,x} + \phi_x) \\
&+ c_z(\delta v_{,x} - \delta u_{,y})\big]\Bigg\}\mathrm{d}A\mathrm{d}t + \int_0^T\int_{\partial R}\Bigg\{\bar{t}_x\delta u + \bar{t}_y\delta v + \bar{t}_z\delta w - \overline{M}_x\delta\phi_x - \overline{M}_y\delta\phi_y \\
&+ \frac{1}{2}\left[\bar{s}_x\delta(w_{,y} + \phi_y) - \bar{s}_y\delta(w_{,x} + \phi_x) + \bar{s}_z(\delta v_{,x} - \delta u_{,y})\right]\Bigg\}\mathrm{d}s\mathrm{d}t,
\end{aligned}
\tag{23}
$$

where f_i and $c_i (i = x, y, z)$ are, respectively, the components of the body force resultant (force per unit area) and the body couple resultant (moment per unit area) through the plate thickness acting in the area R

(i.e., the plate mid-plane), $\bar{t}_i$ and $\bar{s}_i$ $(i = x, y, z)$ are, respectively, the components of the Cauchy traction resultant (force per unit length) and the surface couple resultant (moment per unit length) through the plate thickness acting on ∂R (i.e., the boundary of R), and $\overline{M}_x$ and $\overline{M}_y$ are, respectively, the applied moments per unit length about the y-axis and x-axis acting on ∂R. Note that the positive directions of $\overline{M}_x$ and $\overline{M}_y$ are, respectively, opposite to those of ϕ_x and ϕ_y (see Fig. 1). Also, in reaching Eq. (23), use has been made of Green's theorem.

According to Hamilton's principle (e.g., [19,20,29]),

$$\delta \int_0^T [K - (U - W)]\,\mathrm{d}t = 0. \tag{24}$$

Using Eqs. (14), (16), (18), (21) and (23) in Eq. (24) leads to

$$\begin{aligned}
&\int_0^T \int_R \Bigg[\left(N_{xx,x} + N_{xy,y} + \frac{Y_{xz,xy} + Y_{yz,yy}}{2} - m_0\ddot{u} + f_x + \frac{1}{2}c_{z,y}\right)\delta u \\
&\quad + \left(N_{yy,y} + N_{xy,x} - \frac{Y_{xz,xx} + Y_{yz,xy}}{2} - m_0\ddot{v} + f_y - \frac{1}{2}c_{z,x}\right)\delta v \\
&\quad + \left(N_{xz,x} + N_{yz,y} - \frac{Y_{xx,xy} - Y_{yy,xy} + Y_{xy,yy} - Y_{xy,xx}}{2} - m_0\ddot{w} + f_z - \frac{1}{2}c_{x,y} + \frac{1}{2}c_{y,x}\right)\delta w \\
&\quad - \left(M_{xx,x} + M_{xy,y} - N_{xz} + \frac{H_{yz,yy} + H_{xz,xy} - Y_{zz,y} + Y_{yy,y} + Y_{xy,x}}{2} + m_2\ddot{\phi}_x + \frac{1}{2}c_y\right)\delta\phi_x \\
&\quad - \left(M_{yy,y} + M_{xy,x} - N_{yz} + \frac{Y_{zz,x} - H_{xz,xx} - H_{yz,xy} - Y_{xx,x} - Y_{xy,y}}{2} + m_2\ddot{\phi}_y - \frac{1}{2}c_x\right)\delta\phi_y\Bigg]\mathrm{d}A\mathrm{d}t \\
&\quad - \frac{1}{2}\int_0^T \int_{\partial R} \Bigg\{\left(\frac{1}{2}Y_{xz,x}n_y + \frac{1}{2}Y_{xz,y}n_x + Y_{yz,y}n_y + 2N_{xx}n_x + 2N_{xy}n_y + c_z n_y - 2\bar{t}_x\right)\delta u \\
&\quad - \left(Y_{xz,x}n_x + \frac{1}{2}Y_{yz,x}n_y + \frac{1}{2}Y_{yz,y}n_x - 2N_{yy}n_y - 2N_{xy}n_x + c_z n_x + 2\bar{t}_y\right)\delta v \\
&\quad + \Bigg[-\frac{1}{2}(Y_{xx} - Y_{yy})_{,x}n_y - \frac{1}{2}(Y_{xx} - Y_{yy})_{,y}n_x - Y_{xy,y}n_y + Y_{xy,x}n_x + 2N_{xz}n_x + 2N_{yz}n_y \\
&\quad - c_x n_y + c_y n_x - 2\bar{t}_z\Bigg]\delta w + \Bigg(Y_{zz}n_y - Y_{yy}n_y - Y_{xy}n_x - \frac{1}{2}H_{xz,x}n_y - \frac{1}{2}H_{xz,y}n_x - H_{yz,y}n_y \\
&\quad - 2M_{xx}n_x - 2M_{xy}n_y + 2\overline{M}_x + \bar{s}_y\Bigg)\delta\phi_x + \Big(-Y_{zz}n_x + Y_{xx}n_x + Y_{xy}n_y + H_{xz,x}n_x \\
&\quad + \frac{1}{2}H_{yz,x}n_y + \frac{1}{2}H_{yz,y}n_x - 2M_{yy}n_y - 2M_{xy}n_x + 2\overline{M}_y - \bar{s}_x\Big)\delta\phi_y - \frac{1}{2}Y_{xz}n_y\delta u_{,x} \\
&\quad - \left(\frac{1}{2}Y_{xz}n_x + Y_{yz}n_y - \bar{s}_z\right)\delta u_{,y} + \left(\frac{1}{2}Y_{yz}n_y + Y_{xz}n_x - \bar{s}_z\right)\delta v_{,x} + \frac{1}{2}Y_{yz}n_x\delta v_{,y} \\
&\quad + \left[\frac{1}{2}(Y_{xx} - Y_{yy})n_y - Y_{xy}n_x + \bar{s}_y\right]\delta w_{,x} + \left[\frac{1}{2}(Y_{xx} - Y_{yy})n_x + Y_{xy}n_y - \bar{s}_x\right]\delta w_{,y} \\
&\quad + \frac{1}{2}H_{xz}n_y\delta\phi_{x,x} + \left(\frac{1}{2}H_{xz}n_x + H_{yz}n_y\right)\delta\phi_{x,y} - \left(H_{xz}n_x + \frac{1}{2}H_{yz}n_y\right)\delta\phi_{y,x} \\
&\quad - \frac{1}{2}H_{yz}n_x\delta\phi_{y,y}\Bigg\}\mathrm{d}s\mathrm{d}t = 0.
\end{aligned} \tag{25}$$

Applying the fundamental lemma of the calculus of variations (e.g., [5,31]) to Eq. (25) then gives, with the arbitrariness of δu, δv, δw, $\delta\phi_x$ and $\delta\phi_y$,

$$2N_{xx,x} + 2N_{xy,y} + Y_{xz,xy} + Y_{yz,yy} + 2f_x + c_{z,y} = 2m_0\ddot{u}, \tag{26a}$$

$$2N_{yy,y} + 2N_{xy,x} - Y_{xz,xx} - Y_{yz,xy} + 2f_y - c_{z,x} = 2m_0\ddot{v}, \tag{26b}$$

$$2N_{xz,x} + 2N_{yz,y} - Y_{xx,xy} + Y_{yy,xy} - Y_{xy,yy} + Y_{xy,xx} + 2f_z - c_{x,y} + c_{y,x} = 2m_0\ddot{w}, \tag{26c}$$

$$2M_{xx,x} + 2M_{xy,y} - 2N_{xz} + H_{yz,yy} + H_{xz,xy} - Y_{zz,y} + Y_{yy,y} + Y_{xy,x} + c_y = -2m_2\ddot{\phi}_x, \tag{26d}$$

$$2M_{yy,y} + 2M_{xy,x} - 2N_{yz} + Y_{zz,x} - H_{xz,xx} - H_{yz,xy} - Y_{xx,x} - Y_{xy,y} - c_x = -2m_2\ddot{\phi}_y \tag{26e}$$

as the equations of motion of the Mindlin plate for any $(x, y) \in R$ and $t \in (0, T)$, and

$$\begin{aligned}
&-\frac{1}{2}\int_0^T\int_{\partial R}\left\{\left(\frac{1}{2}Y_{xz,x}n_y + \frac{1}{2}Y_{xz,y}n_x + Y_{yz,y}n_y + 2N_{xx}n_x + 2N_{xy}n_y + c_z n_y - 2\bar{t}_x\right)\delta u\right.\\
&-\left(Y_{xz,x}n_x + \frac{1}{2}Y_{yz,x}n_y + \frac{1}{2}Y_{yz,y}n_x - 2N_{yy}n_y - 2N_{xy}n_x + c_z n_x + 2\bar{t}_y\right)\delta v\\
&+\left[-\frac{1}{2}(Y_{xx} - Y_{yy})_{,x}n_y - \frac{1}{2}(Y_{xx} - Y_{yy})_{,y}n_x - Y_{xy,y}n_y + Y_{xy,x}n_x + 2N_{xz}n_x + 2N_{yz}n_y\right.\\
&\left.-c_x n_y + c_y n_x - 2\bar{t}_z\right]\delta w + \left(Y_{zz}n_y - Y_{yy}n_y - Y_{xy}n_x - \frac{1}{2}H_{xz,x}n_y - \frac{1}{2}H_{xz,y}n_x - H_{yz,y}n_y\right.\\
&\left.-2M_{xx}n_x - 2M_{xy}n_y + 2\overline{M}_x + \bar{s}_y\right)\delta\phi_x + \left(-Y_{zz}n_x + Y_{xx}n_x + Y_{xy}n_y + H_{xz,x}n_x\right.\\
&\left.+\frac{1}{2}H_{yz,x}n_y + \frac{1}{2}H_{yz,y}n_x - 2M_{yy}n_y - 2M_{xy}n_x + 2\overline{M}_y - \bar{s}_x\right)\delta\phi_y - \frac{1}{2}Y_{xz}n_y\delta u_{,x}\\
&-\left(\frac{1}{2}Y_{xz}n_x + Y_{yz}n_y - \bar{s}_z\right)\delta u_{,y} + \left(\frac{1}{2}Y_{yz}n_y + Y_{xz}n_x - \bar{s}_z\right)\delta v_{,x} + \frac{1}{2}Y_{yz}n_x\delta v_{,y}\\
&+\left[\frac{1}{2}(Y_{xx} - Y_{yy})n_y - Y_{xy}n_x + \bar{s}_y\right]\delta w_{,x} + \left[\frac{1}{2}(Y_{xx} - Y_{yy})n_x + Y_{xy}n_y - \bar{s}_x\right]\delta w_{,y}\\
&+\frac{1}{2}H_{xz}n_y\delta\phi_{x,x} + \left(\frac{1}{2}H_{xz}n_x + H_{yz}n_y\right)\delta\phi_{x,y} - \left(H_{xz}n_x + \frac{1}{2}H_{yz}n_y\right)\delta\phi_{y,x}\\
&\left.-\frac{1}{2}H_{yz}n_x\delta\phi_{y,y}\right\}\mathrm{d}s\mathrm{d}t = 0,
\end{aligned} \tag{26f}$$

which can be further simplified to obtain the boundary conditions.

Note that the integrand of the line integral in Eq. (26f) is expressed in terms of the Cartesian components of the resultants and displacements that are functions of the Cartesian coordinates (x, y, z) with the unit base vectors $\{\mathbf{e}_1, \mathbf{e}_2, \mathbf{e}_3\}$. This is convenient for a rectangular plate whose edges are parallel to the x- and y-axes. However, for a more general case of a plate whose boundary is not aligned with the x- or y-axis, as shown in Fig. 2, it is more convenient to use a Cartesian coordinate system (n, s, z) with the unit base vectors $\{\mathbf{e}_n, \mathbf{e}_s, \mathbf{e}_3\}$, where $\mathbf{e}_n(= n_x\mathbf{e}_1 + n_y\mathbf{e}_2)$ and $\mathbf{e}_s(= -n_y\mathbf{e}_1 + n_x\mathbf{e}_2)$ are, respectively, the unit normal and tangent vectors on the plate boundary ∂R.

It can be shown that the components in the coordinate system (x, y, z) are related to those in the coordinate system (n, s, z) through the following transformation expressions:

$$\begin{aligned}
&\{u,\ v\}^T = [R_1]\{u_n,\ u_s\}^T, \quad \{\phi_x,\ \phi_y\}^T = [R_1]\{\phi_n,\ \phi_s\}^T, \quad \{w_{,x},\ w_{,y}\}^T = [R_1]\{w_{,n},\ w_{,s}\}^T,\\
&\{N_{xz},\ N_{yz}\}^T = [R_1]\{N_{nz},\ N_{sz}\}^T, \quad \{\bar{t}_x,\ \bar{t}_y\}^T = [R_1]\{\bar{t}_n,\ \bar{t}_s\}^T, \quad \{\bar{s}_x,\ \bar{s}_y\}^T = [R_1]\{\bar{s}_n,\ \bar{s}_s\}^T,\\
&\{\bar{c}_x,\ \bar{c}_y\}^T = [R_1]\{\bar{c}_n,\ \bar{c}_s\}^T, \quad \{\overline{M}_x,\ \overline{M}_y\}^T = [R_1]\{\overline{M}_n,\ \overline{M}_s\}^T,\\
&\{Y_{xz},\ Y_{yz}\}^T = [R_1]\{Y_{nz},\ Y_{sz}\}^T, \quad \{H_{xz},\ H_{yz}\}^T = [R_1]\{H_{nz},\ H_{sz}\}^T,\\
&\begin{Bmatrix} N_{xx} & N_{xy}\\ N_{xy} & N_{yy}\end{Bmatrix} = [R_1]\begin{Bmatrix} N_{nn} & N_{ns}\\ N_{ns} & N_{ss}\end{Bmatrix}[R_1]^T, \quad \begin{Bmatrix} Y_{xx} & Y_{xy}\\ Y_{xy} & Y_{yy}\end{Bmatrix} = [R_1]\begin{Bmatrix} Y_{nn} & Y_{ns}\\ Y_{ns} & Y_{ss}\end{Bmatrix}[R_1]^T,
\end{aligned}$$

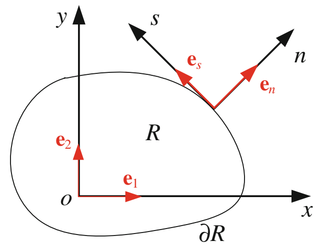

Fig. 2 Two coordinate systems

$$\begin{Bmatrix} M_{xx} & M_{xy} \\ M_{xy} & M_{yy} \end{Bmatrix} = [R_1] \begin{Bmatrix} M_{nn} & M_{ns} \\ M_{ns} & M_{ss} \end{Bmatrix} [R_1]^T, \quad \begin{Bmatrix} u_{,x} & u_{,y} \\ v_{,x} & v_{,y} \end{Bmatrix} = [R_1] \begin{Bmatrix} u_{n,n} & u_{n,s} \\ v_{s,n} & v_{s,s} \end{Bmatrix} [R_1]^T,$$
$$\begin{Bmatrix} \phi_{x,x} & \phi_{x,y} \\ \phi_{y,x} & \phi_{y,y} \end{Bmatrix} = [R_1] \begin{Bmatrix} \phi_{n,n} & \phi_{n,s} \\ \phi_{s,n} & \phi_{s,s} \end{Bmatrix} [R_1]^T, \quad \begin{Bmatrix} H_{xz,x} & H_{xz,y} \\ H_{yz,x} & H_{yz,y} \end{Bmatrix} = [R_1] \begin{Bmatrix} H_{nz,n} & H_{nz,s} \\ H_{sz,n} & H_{sz,s} \end{Bmatrix} [R_1]^T,$$
$$\begin{Bmatrix} Y_{xz,x} & Y_{xz,y} \\ Y_{yz,x} & Y_{yz,y} \end{Bmatrix} = [R_1] \begin{Bmatrix} Y_{nz,n} & Y_{nz,s} \\ Y_{sz,n} & Y_{sz,s} \end{Bmatrix} [R_1]^T,$$
$$\left[Y_{xx,x},\ Y_{xx,y},\ Y_{xy,x},\ Y_{xy,y},\ Y_{yy,x},\ Y_{yy,y}\right]^T = [R_3]\left[Y_{nn,n},\ Y_{nn,s},\ Y_{ns,n},\ Y_{ns,s},\ Y_{ss,n},\ Y_{ss,s}\right]^T, \tag{27}$$

where

$$[R_1] \equiv \begin{Bmatrix} n_x & -n_y \\ n_y & n_x \end{Bmatrix},$$
$$[R_3] = \begin{bmatrix} n_x^3 & -n_x^2 n_y & -2n_x^2 n_y & 2n_x n_y^2 & n_x n_y^2 & -n_y^3 \\ n_x^2 n_y & n_x^3 & -2n_x n_y^2 & -2n_x^2 n_y & n_y^3 & n_x n_y^2 \\ n_x^2 n_y & -n_x n_y^2 & n_x(n_x^2 - n_y^2) & -n_y(n_x^2 - n_y^2) & -n_x^2 n_y & n_x n_y^2 \\ n_x n_y^2 & n_x^2 n_y & n_y(n_x^2 - n_y^2) & n_x(n_x^2 - n_y^2) & -n_x n_y^2 & -n_x^2 n_y \\ n_x n_y^2 & -n_y^3 & 2n_x^2 n_y & -2n_x n_y^2 & n_x^3 & -n_x^2 n_y \\ n_y^3 & n_x n_y^2 & 2n_x n_y^2 & 2n_x^2 n_y & n_x^2 n_y & n_x^3 \end{bmatrix}, \tag{28}$$

with $n_x^2 + n_y^2 = 1$.

Using Eqs. (27) and (28) in Eq. (26f) gives

$$\begin{aligned} &\int_0^T \int_{\partial R} \Bigg\{ \left(2N_{nn} + \frac{1}{2}Y_{nz,s} - 2\bar{t}_n\right)\delta u_n - \left(-2N_{ns} + Y_{nz,n} + \frac{Y_{sz,s}}{2} + c_z + 2\bar{t}_s\right)\delta u_s \\ &+ \left(\frac{Y_{ss,s} - Y_{nn,s}}{2} + Y_{ns,n} + 2N_{nz} + c_s - 2\bar{t}_3\right)\delta w + (-Y_{ns} + \bar{s}_s)\delta w_{,n} + \left(\frac{Y_{nn} - Y_{ss}}{2} - \bar{s}_n\right)\delta w_{,s} \\ &+ \left(-\frac{1}{2}H_{nz,s} - Y_{ns} - 2M_{nn} + 2\overline{M}_n + \bar{s}_s\right)\delta\phi_n + \Bigg(H_{nz,n} + \frac{H_{sz,s}}{2} - Y_{zz} + Y_{nn} - 2M_{ns} \\ &+ 2\overline{M}_s - \bar{s}_n\Bigg)\delta\phi_s + \left(-\frac{Y_{nz}}{2} + \bar{s}_z\right)\delta u_{n,s} + (Y_{nz} - \bar{s}_z)\delta u_{s,n} + \frac{Y_{sz}}{2}\delta u_{s,s} + \frac{H_{nz}}{2}\delta\phi_{n,s} \\ &- H_{nz}\delta\phi_{s,n} - \frac{H_{sz}}{2}\delta\phi_{s,s}\Bigg\}\, \mathrm{d}s\mathrm{d}t = 0. \end{aligned} \tag{29}$$

Note that on the closed boundary ∂R, the following identity:

$$\int_{\partial R} F\delta g_{,s}\mathrm{d}s = -\int_{\partial R} F_{,s}\delta g\mathrm{d}s \tag{30}$$

holds. The use of Eq. (30) in Eq. (29) results in

$$\int_0^T \int_{\partial R} (\hat{\mathrm{N}}_{nn}\delta u_n + \hat{\mathrm{N}}_{ss}\delta u_s + \hat{\mathrm{N}}_{zz}\delta w + \hat{\mathrm{M}}_n\delta\phi_n + \hat{\mathrm{M}}_s\delta\phi_s + \hat{\mathrm{T}}_z\delta w_{,n} + \hat{\mathrm{T}}_s\delta u_{s,n} + \hat{\mathrm{Z}}_s\delta\phi_{s,n})\mathrm{d}s\mathrm{d}t = 0, \quad (31)$$

where

$$\hat{\mathrm{N}}_{nn} \equiv 2N_{nn} + Y_{nz,s} - 2\bar{t}_n - \bar{s}_{z,s}, \quad (32a)$$
$$\hat{\mathrm{N}}_{ss} \equiv 2N_{ns} - Y_{nz,n} - Y_{sz,s} - c_z - 2\bar{t}_s, \quad (32b)$$
$$\hat{\mathrm{N}}_{zz} \equiv 2N_{nz} + Y_{ss,s} - Y_{nn,s} + Y_{ns,n} + c_s - 2\bar{t}_z + \bar{s}_{n,s}, \quad (32c)$$
$$\hat{\mathrm{M}}_n \equiv -2M_{nn} - H_{nz,s} - Y_{ns} + 2\overline{M}_n + \bar{s}_s, \quad (32d)$$
$$\hat{\mathrm{M}}_s \equiv -2M_{ns} + H_{nz,n} + H_{sz,s} - Y_{zz} + Y_{nn} + 2\overline{M}_s - \bar{s}_n, \quad (32e)$$
$$\hat{\mathrm{T}}_z \equiv -Y_{ns} + \bar{s}_s, \quad (32f)$$
$$\hat{\mathrm{T}}_s \equiv Y_{nz} - \bar{s}_z, \quad (32g)$$
$$\hat{\mathrm{Z}}_s \equiv -H_{nz}. \quad (32h)$$

With the help of the fundamental lemma of the calculus of variations, Eq. (31) yields

$$\hat{\mathrm{N}}_{nn} = 0 \quad \text{or} \quad u_n = \bar{u}_n, \quad (33a)$$
$$\hat{\mathrm{N}}_{ss} = 0 \quad \text{or} \quad u_s = \bar{u}_s, \quad (33b)$$
$$\hat{\mathrm{N}}_{zz} = 0 \quad \text{or} \quad w = \bar{w}, \quad (33c)$$
$$\hat{\mathrm{M}}_n = 0 \quad \text{or} \quad \phi_n = \bar{\phi}_n, \quad (33d)$$
$$\hat{\mathrm{M}}_s = 0 \quad \text{or} \quad \phi_s = \bar{\phi}_s, \quad (33e)$$
$$\hat{\mathrm{T}}_z = 0 \quad \text{or} \quad w_{,n} = \overline{w_{,n}}, \quad (33f)$$
$$\hat{\mathrm{T}}_s = 0 \quad \text{or} \quad u_{s,n} = \overline{u_{s,n}}, \quad (33g)$$
$$\hat{\mathrm{Z}}_s = 0 \quad \text{or} \quad \phi_{s,n} = \bar{\phi}_{s,n} \quad (33h)$$

as the boundary conditions for any $(x, y) \in \partial R$ and $t \in (0, T)$, where the overbar represents the prescribed value.

From Eqs. (5), (11), and (17a–17h), the stress resultants can be expressed in terms of u, v, w, ϕ_x and ϕ_y as

$$N_{xx} = h[(\lambda + 2\mu)u_{,x} + \lambda v_{,y}], \quad (34a)$$
$$N_{yy} = h[(\lambda + 2\mu)v_{,y} + \lambda u_{,x}], \quad (34b)$$
$$N_{xz} = k_s h\mu(w_{,x} - \phi_x), \quad (34c)$$
$$N_{yz} = k_s h\mu(w_{,y} - \phi_y), \quad (34d)$$
$$N_{xy} = h\mu(u_{,y} + v_{,x}), \quad (34e)$$
$$M_{xx} = -\frac{h^3}{12}\left[(\lambda + 2\mu)\phi_{x,x} + \lambda\phi_{y,y}\right], \quad (34f)$$
$$M_{yy} = -\frac{h^3}{12}\left[(\lambda + 2\mu)\phi_{y,y} + \lambda\phi_{x,x}\right], \quad (34g)$$
$$M_{xy} = -\frac{h^3}{12}\mu\left(\phi_{x,y} + \phi_{y,x}\right), \quad (34h)$$

where k_s is a shear correction factor introduced to account for the non-uniformity of the shear strain components ε_{xz} and ε_{yz} over the plate thickness (e.g., [32–35]).

Also, from Eqs. (6), (13) and (19), the couple stress resultants can be expressed in terms of u, v, w, ϕ_x and ϕ_y as

$$Y_{xx} = hl^2\mu(w_{,xy} + \phi_{y,x}), \tag{35a}$$
$$Y_{yy} = -hl^2\mu(w_{,xy} + \phi_{x,y}), \tag{35b}$$
$$Y_{zz} = hl^2\mu(-\phi_{y,x} + \phi_{x,y}), \tag{35c}$$
$$Y_{xy} = \frac{1}{2}l^2\mu h(w_{,yy} + \phi_{y,y} - w_{,xx} - \phi_{x,x}), \tag{35d}$$
$$Y_{xz} = \frac{1}{2}l^2\mu h\left(v_{,xx} - u_{,xy}\right), \tag{35e}$$
$$Y_{yz} = \frac{1}{2}l^2\mu h\left(v_{,xy} - u_{,yy}\right), \tag{35f}$$
$$H_{xz} = \frac{1}{24}\mu l^2 h^3\left(-\phi_{y,xx} + \phi_{x,xy}\right), \tag{35g}$$
$$H_{yz} = \frac{1}{24}\mu l^2 h^3\left(-\phi_{y,xy} + \phi_{x,yy}\right). \tag{35h}$$

The involvement of Y_{xx}, Y_{yy}, Y_{zz}, Y_{xy}, Y_{xz}, Y_{yz}, H_{xz} and H_{yz} in the current model (see Eqs. (26a–26e)) is a direct result of including the couple stress contribution to the strain energy of the plate. As shown in Eqs. (35a–35h), these couple stress resultants explicitly depend on the material length scale parameter l and all vanish when $l = 0$ (i.e., when the couple stress effect is not considered).

By using Eqs. (22), (34a–34h) and (35a–35h) in Eqs. (26a–26e), the equations of motion of the Mindlin plate in terms of u, v, w, ϕ_x and ϕ_y can be obtained as

$$(\lambda + 2\mu)u_{,xx} + \mu u_{,yy} + (\lambda + \mu)v_{,xy} + \frac{1}{4}l^2\mu\left(-u_{,xxyy} - u_{,yyyy} + v_{,xxxy} + v_{,xyyy}\right) + \frac{1}{h}\left(f_x + \frac{1}{2}c_{z,y}\right) = \rho\ddot{u}, \tag{36a}$$

$$(\lambda + 2\mu)v_{,yy} + \mu v_{,xx} + (\lambda + \mu)u_{,xy} + \frac{1}{4}l^2\mu\left(u_{,xxxy} + u_{,xyyy} - v_{,xxxx} - v_{,xxyy}\right) + \frac{1}{h}\left(f_y - \frac{1}{2}c_{z,x}\right) = \rho\ddot{v}, \tag{36b}$$

$$k_s\mu(w_{,xx} + w_{,yy} - \phi_{x,x} - \phi_{y,y}) - \frac{1}{4}l^2\mu(w_{,xxxx} + 2w_{,xxyy} + w_{,yyyy} + \phi_{x,xxx} + \phi_{x,xyy} + \phi_{y,xxy} + \phi_{y,yyy}) + \frac{1}{h}\left(f_z - \frac{1}{2}c_{x,y} + \frac{1}{2}c_{y,x}\right) = \rho\ddot{w}, \tag{36c}$$

$$(\lambda + 2\mu)\phi_{x,xx} + \mu\phi_{x,yy} + (\lambda + \mu)\phi_{y,xy} + \frac{12k_s\mu}{h^2}(w_{,x} - \phi_x) + \frac{l^2\mu}{4}(-\phi_{x,xxyy} - \phi_{x,yyyy} + \phi_{y,xxxy} + \phi_{y,xyyy}) - \frac{3l^2\mu}{h^2}(-w_{,xxx} - w_{,xyy} - \phi_{x,xx} - 4\phi_{x,yy} + 3\phi_{y,xy}) - \frac{6c_y}{h^3} = \rho\ddot{\phi}_x, \tag{36d}$$

$$(\lambda + \mu)\phi_{x,xy} + \mu\phi_{y,xx} + (\lambda + 2\mu)\phi_{y,yy} + \frac{12k_s\mu}{h^2}(w_{,y} - \phi_y) + \frac{l^2\mu}{4}(\phi_{x,xxxy} + \phi_{x,xyyy} - \phi_{y,xxxx} - \phi_{y,xxyy}) - \frac{3l^2\mu}{h^2}\left(-w_{,xxy} - w_{,yyy} + 3\phi_{x,xy} - 4\phi_{y,xx} - \phi_{y,yy}\right) + \frac{6c_x}{h^3} = \rho\ddot{\phi}_y \tag{36e}$$

for any $(x, y) \in R$ and $t \in (0, T)$.

The differential equations in Eqs. (36a–36e), the boundary conditions in Eqs. (33a–33h) (along with Eqs. (27), (32a–32h), (34a–34h) and (35a–35h)), and given initial conditions at $t = 0$ and $t = T$ form a boundary-initial value problem for determining u, v, w, ϕ_x and ϕ_y. It is observed from Eqs. (36a–36e) that the in-plane displacements u and v are uncoupled with the out-of-plane displacement w and the rotations ϕ_x and ϕ_y and can therefore be obtained separately from solving Eqs. (36a, 36b) subject to prescribed boundary conditions of the form in Eqs. (33a, 33b, 33g) and suitable initial conditions.

When $v=0$, $\phi_y=0$, $u=u(x,t)$, $w=w(x,t)$, $\phi_x=\phi_x(x,t)$, $f_y=0$, $c_x=0$ and $c_z=0$, the Mindlin plate considered here becomes the Timoshenko beam studied in Ma et al. [19]. For this case, Eqs. (36a–36e) reduce to

$$\frac{E(1-\nu)h}{(1+\nu)(1-2\nu)}\frac{\partial^2 u}{\partial x^2}+f_x=m_o\frac{\partial^2 u}{\partial t^2}, \tag{37a}$$

$$k_s\mu h\left(-\frac{\partial\phi_x}{\partial x}+\frac{\partial^2 w}{\partial x^2}\right)-\frac{1}{4}l^2\mu h\left(\frac{\partial^3\phi_x}{\partial x^3}+\frac{\partial^4 w}{\partial x^4}\right)+\frac{1}{2}\frac{\partial c_y}{\partial x}+f_z=m_o\frac{\partial^2 w}{\partial t^2}, \tag{37b}$$

$$\frac{E(1-\nu)}{(1+\nu)(1-2\nu)}\frac{h^3}{12}\frac{\partial^2\phi_x}{\partial x^2}+k_s\mu h(-\phi_x+\frac{\partial w}{\partial x})+\frac{1}{4}l^2\mu h\left(\frac{\partial^2\phi_x}{\partial x^2}+\frac{\partial^3 w}{\partial x^3}\right)-\frac{1}{2}c_y=m_2\frac{\partial^2\phi_x}{\partial t^2} \tag{37c}$$

for any $x\in(0,L)$ and $t\in(0,T)$, where L is the length of the beam (plate). In reaching Eqs. (37a–37c), use has been made of Eqs. (7) and (22). The governing equations in Eqs. (37a–37c) are identical to those derived in [19] for the Timoshenko beam with a unit width and a height h. That is, the current Mindlin plate model recovers the non-classical Timoshenko beam model based on the same modified couple stress theory.

Also, the current non-classical Mindlin plate model can be reduced to that based on classical elasticity, as shown below. In the classical Mindlin plate theory for transversely inextensible plates (e.g., [33,36]), the following constitutive equations are used (e.g., [35]):

$$\sigma_{xx}=\frac{E}{1-\nu^2}(\varepsilon_{xx}+\nu\varepsilon_{yy}),\quad \sigma_{yy}=\frac{E}{1-\nu^2}(\varepsilon_{yy}+\nu\varepsilon_{xx}),\quad \tau_{xy}=\frac{E}{2(1+\upsilon)}\gamma_{xy}. \tag{38}$$

Clearly, the plane stress expressions listed in Eq. (38) are different from those given in Eq. (5) based on the three-dimensional Hooke's law.

From Eqs. (11), (17a, 17b, 17f, 17g) and (38), it follows that

$$N_{xx}=\frac{Eh}{1-\nu^2}(u_{,x}+\nu v_{,y}),\quad N_{yy}=\frac{Eh}{1-\nu^2}(v_{,y}+\nu u_{,x}),$$
$$M_{xx}=-\frac{E}{12(1-\nu^2)}h^3(\phi_{x,x}+\nu\phi_{y,y}),\quad M_{yy}=-\frac{E}{12(1-\nu^2)}h^3(\phi_{y,y}+\nu\phi_{x,x}), \tag{39}$$

while the expressions of the other Cauchy stress resultants N_{xz}, N_{yz}, N_{xy} and M_{xy} in Eqs. (34c–34e, 34h) remain unchanged.

After using Eqs. (39), (34c–34e, 34h) and (22) and the fact that the couple stress resultants in Eqs. (35a–35h) all vanish when $l=0$, Eqs. (26a–26e) become, with $c_x=c_y=c_z=0$,

$$\frac{E}{1-\nu^2}(u_{,xx}+\nu v_{,xy})+\mu(u_{,yy}+v_{,xy})+\frac{f_x}{h}=\rho\ddot{u}, \tag{40a}$$

$$\frac{E}{1-\nu^2}(v_{,yy}+\nu u_{,xy})+\mu(u_{,xy}+v_{,xx})+\frac{f_y}{h}=\rho\ddot{v}, \tag{40b}$$

$$k_s\mu(w_{,xx}-\phi_{x,x}+w_{,yy}-\phi_{y,y})+\frac{f_z}{h}=\rho\ddot{w}, \tag{40c}$$

$$-\frac{h^2}{12}\left[\frac{E}{1-\nu^2}(\phi_{x,xx}+\nu\phi_{y,xy})+\mu(\phi_{x,yy}+\phi_{y,xy})\right]-k_s\mu(w_{,x}-\phi_x)=-\frac{h^2}{12}\rho\ddot{\phi}_x, \tag{40d}$$

$$-\frac{h^2}{12}\left[\frac{E}{1-\nu^2}(\phi_{y,yy}+\nu\phi_{x,xy})+\mu(\phi_{x,xy}+\phi_{y,xx})\right]-k_s\mu(w_{,y}-\phi_y)=-\frac{h^2}{12}\rho\ddot{\phi}_y \tag{40e}$$

for any $(x,y)\in R$ and $t\in(0,T)$. These are the governing equations for the Mindlin plate satisfying the general kinematic relations in Eq. (10) based on classical elasticity.

For a Timoshenko beam with $v=0$, $\phi_y=0$, $u=u(x,t)$, $w=w(x,t)$, $\phi_x=\phi_x(x,t)$, $f_y=0$ and with the Poisson effect ignored by setting $\nu=0$, Eqs. (40a–40e) reduce to

$$Eh\frac{\partial^2 u}{\partial x^2}+f_x=m_o\frac{\partial^2 u}{\partial t^2}, \tag{41a}$$

$$k_s\mu h(-\frac{\partial\phi_x}{\partial x}+\frac{\partial^2 w}{\partial x^2})+f_z=m_o\frac{\partial^2 w}{\partial t^2}, \tag{41b}$$

$$\frac{Eh^3}{12}\frac{\partial^2\phi_x}{\partial x^2}+k_s\mu h(-\phi_x+\frac{\partial w}{\partial x})=m_2\frac{\partial^2\phi_x}{\partial t^2}, \tag{41c}$$

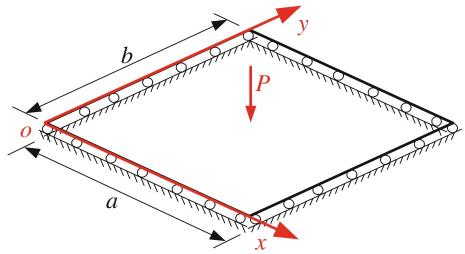

Fig. 3 Simply supported plate

where use has been made of Eq. (22). The governing equations in Eqs. (41a–41c) are the same as those provided in [19] for the Timoshenko beam with a unit width and a height h based on classical elasticity.

3 Examples: static bending and free vibration of a simply supported plate

To further illustrate the non-classical Mindlin plate model developed in Sect. 2, the static bending and free vibration problems of a simply supported rectangular plate (see Fig. 3) are analytically solved here by directly applying the general forms of the governing equations and boundary conditions of the new model.

In view of Eqs. (33a–33h), the boundary conditions of this simply supported plate can be identified as

$$u_s = 0, \quad \phi_s = 0, \quad w = 0, \quad \hat{\mathrm{N}}_{nn} = 0, \quad \hat{\mathrm{M}}_n = 0, \quad \hat{\mathrm{T}}_z = 0, \quad \hat{\mathrm{T}}_s = 0, \quad \hat{\mathrm{Z}}_s = 0 \tag{42}$$

for all (x, y) on the boundaries $x = 0, a$ and $y = 0, b$. Also, the following applied traction resultants vanish on these boundaries:

$$\bar{s}_s = \bar{s}_z = \bar{s}_{z,s} = 0, \quad \bar{t}_n = 0, \quad \overline{M}_n = 0. \tag{43}$$

For the boundaries $x = 0$ and $x = a$, $n_y = 0$ and $n_x = -1$ (on $x = 0$) or $n_x = 1$ (on $x = a$). With the help of Eqs. (27), (32a–32h) and (43), Eq. (42) becomes

$$v(0, y) = v(a, y) = 0, \tag{44a}$$
$$w(0, y) = w(a, y) = 0, \tag{44b}$$
$$\phi_y(0, y) = \phi_y(a, y) = 0, \tag{44c}$$
$$2N_{xx} + Y_{xz.y} = 0 \text{ on } x = 0 \quad \text{and} \quad x = a, \tag{44d}$$
$$2M_{xx} + H_{xz.y} + Y_{xy} = 0 \text{ on } x = 0 \quad \text{and} \quad x = a, \tag{44e}$$
$$Y_{xy} = 0 \text{ on } x = 0 \quad \text{and} \quad x = a, \tag{44f}$$
$$Y_{xz} = 0 \text{ on } x = 0 \quad \text{and} \quad x = a, \tag{44g}$$
$$H_{xz} = 0 \text{ on } x = 0 \quad \text{and} \quad x = a. \tag{44h}$$

Using Eqs. (34a–34h) and (35a–35h) in Eqs. (44d–44h) gives

$$2\left[(\lambda + 2\mu)u_{,x} + \lambda v_{,y}\right] + \frac{1}{2}l^2\mu\left(v_{,xxy} - u_{,xyy}\right) = 0, \tag{45a}$$

$$-\frac{h^2}{6}\left[(\lambda + 2\mu)\phi_{x,x} + \lambda\phi_{y,y}\right] + \frac{1}{24}\mu l^2 h^2\left(-\phi_{y,xxy} + \phi_{x,xyy}\right) + \frac{1}{2}\mu l^2(w_{,yy} + \phi_{y,y} - w_{,xx} - \phi_{x,x}) = 0, \tag{45b}$$

$$w_{,yy} + \phi_{y,y} - w_{,xx} - \phi_{x,x} = 0, \tag{45c}$$
$$v_{,xx} - u_{,xy} = 0, \tag{45d}$$
$$-\phi_{y,xx} + \phi_{x,xy} = 0 \tag{45e}$$

on $x = 0$ and $x = a$.

For the boundaries $y = 0$ and $y = b$, $n_x = 0$ and $n_y = -1$ (on $y = 0$) or $n_y = 1$ (on $y = b$). With the help of Eqs. (27), (32a–32h) and (43), Eq. (42) now becomes

$$u(x, 0) = u(x, b) = 0, \tag{46a}$$
$$w(x, 0) = w(x, b) = 0, \tag{46b}$$
$$\phi_x(x, 0) = \phi_x(x, b) = 0, \tag{46c}$$
$$2N_{yy} - Y_{yz,x} = 0 \text{ on } y = 0 \text{ and } y = b, \tag{46d}$$
$$-2M_{yy} + H_{yz,x} + Y_{xy} = 0 \text{ on } y = 0 \text{ and } y = b, \tag{46e}$$
$$Y_{xy} = 0 \text{ on } y = 0 \text{ and } y = b, \tag{46f}$$
$$Y_{yz} = 0 \text{ on } y = 0 \text{ and } y = b, \tag{46g}$$
$$H_{yz} = 0 \text{ on } y = 0 \text{ and } y = b. \tag{46h}$$

The use of Eqs. (34a–34h) and (35a–35h) in Eqs. (46d–46h) yields

$$2\left[(\lambda + 2\mu)v_{,y} + \lambda u_{,x}\right] - \frac{1}{2}\mu l^2 \left(v_{,xxy} - u_{,xyy}\right) = 0, \tag{47a}$$
$$\frac{h^2}{6}\left[\lambda\phi_{x,x} + (\lambda + 2\mu)\phi_{y,y}\right] + \frac{1}{24}l^2\mu h^2\left(-\phi_{y,xxy} + \phi_{x,xyy}\right) + \frac{1}{2}\mu l^2(w_{,yy} + \phi_{y,y} - w_{,xx} - \phi_{x,x}) = 0, \tag{47b}$$
$$w_{,yy} + \phi_{y,y} - w_{,xx} - \phi_{x,x} = 0, \tag{47c}$$
$$v_{,xy} - u_{,yy} = 0, \tag{47d}$$
$$-\phi_{y,xy} + \phi_{x,yy} = 0 \tag{47e}$$

on $y = 0$ and $y = b$.

3.1 Static bending

For static bending problems, u, v, w, ϕ_x and ϕ_y are independent of time t such that $u = u(x, y)$, $v = v(x, y)$, $w = w(x, y)$, $\phi_x = \phi_x(x, y)$ and $\phi_y = \phi_y(x, y)$. As a result, all of the time derivatives involved in Eqs. (36a–36e) vanish.

The boundary value problem (BVP) for the static bending of the simply supported plate shown in Fig. 3 is defined by Eqs. (36a–36e), (44a–44c), (45a–45e), (46a–46c) and (47a–47e), with $u = u(x, y)$, $v = v(x, y)$, $w = w(x, y)$, $\phi_x = \phi_x(x, y)$ and $\phi_y = \phi_y(x, y)$. As mentioned in Sect. 2, the in-plane displacements u and v are uncoupled with w, ϕ_x and ϕ_y. They can be obtained from solving the BVP defined by Eqs. (36a, 36b), (44a), (45a, 45d), (46a) and (47a, 47d). For the current case with $f_x = f_y = 0$ and $c_z = 0$, the solution of this BVP gives $u = v = 0$ for any $(x, y) \in R$.

The out-of-plane displacement w and the rotations ϕ_x and ϕ_y can be obtained from solving the BVP defined by Eqs. (36c–36e), (44b, 44c), (45b, 45c, 45e), (46b, 46c) and (47b, 47c, 47e).

Consider the following Fourier series solutions for w, ϕ_x and ϕ_y:

$$w = \sum_{m=1}^{\infty}\sum_{n=1}^{\infty} W_{mn} \sin\left(\frac{m\pi x}{a}\right)\sin\left(\frac{n\pi y}{b}\right), \quad \phi_x = \sum_{m=1}^{\infty}\sum_{n=1}^{\infty} \Phi_{mn}^{x} \cos\left(\frac{m\pi x}{a}\right)\sin\left(\frac{n\pi y}{b}\right),$$
$$\phi_y = \sum_{m=1}^{\infty}\sum_{n=1}^{\infty} \Phi_{mn}^{y} \sin\left(\frac{m\pi x}{a}\right)\cos\left(\frac{n\pi y}{b}\right), \tag{48}$$

where W_{mn}, Φ_{mn}^x, and Φ_{mn}^y are Fourier coefficients to be determined for each pair of m and n. Clearly, the expansions in Eq. (48) satisfy the boundary conditions in Eqs. (44b, 44c), (45b, 45c, 45e) at $x = 0, a$ and in Eqs. (46b, 46c), (47b, 47c, 47e) at $y = 0, b$ for any W_{mn}, Φ_{mn}^x and Φ_{mn}^y.

The resultant force $f_z(x, y)$ can also be expanded in a Fourier series as

$$f_z(x, y) = \sum_{m=1}^{\infty}\sum_{n=1}^{\infty} Q_{mn} \sin\left(\frac{m\pi x}{a}\right) \sin\left(\frac{n\pi y}{b}\right), \tag{49}$$

where the Fourier coefficient Q_{mn} is given by

$$Q_{mn} = \frac{4}{ab}\int_0^a\int_0^b f_z(x, y) \sin\left(\frac{m\pi x}{a}\right) \sin\left(\frac{n\pi y}{b}\right) \mathrm{d}x\mathrm{d}y. \tag{50}$$

In the current case, $f_z(x, y) = P\delta\big(x - \frac{a}{2}\big)\delta\big(y - \frac{b}{2}\big)$, where $\delta(\cdot)$ is the Dirac delta function. Using this $f_z(x, y)$ in Eq. (50) then gives

$$Q_{mn} = \frac{4P}{ab} \sin\left(\frac{m\pi}{2}\right) \sin\left(\frac{n\pi}{2}\right). \tag{51}$$

Substituting Eq. (48) into Eqs. (36c–36e) leads to, with $c_x = c_y = 0$,

$$[C]\,[W_{mn},\ \Phi^x_{mn},\ \Phi^y_{mn}]^T = \left[-\frac{Q_{mn}}{h},\ 0,\ 0\right]^T, \tag{52}$$

where $[C]$ is a 3-by-3 matrix whose components are

$$\begin{aligned}
C_{11} &= -\frac{k_s\mu}{a^2b^2}\pi^2(a^2n^2 + b^2m^2) - \frac{\mu}{4a^2b^4}l^2\pi^4n^2(a^2n^2 + 2b^2m^2),\\
C_{12} &= \frac{k_s\mu}{a}\pi m - \frac{\mu m}{4a^3b^2}l^2\pi^3(a^2n^2 + b^2m^2),\quad C_{13} = \frac{k_s\mu}{b}\pi n - \frac{\mu n}{4a^2b^3}l^2\pi^3(a^2n^2 + b^2m^2),\\
C_{22} &= -\frac{12k_s\mu}{h^2} - \frac{1}{a^2b^2}\pi^2[(\lambda + 2\mu)b^2m^2 + \mu a^2n^2]\\
&\quad - \frac{\mu}{4a^2b^4h^2}l^2\pi^2[h^2\pi^2n^2(a^2n^2 + b^2m^2) + 12b^2(4a^2n^2 + b^2m^2)],\\
C_{23} &= -\frac{mn}{ab}\pi^2(\lambda + \mu) + \frac{\mu mn}{4a^3b^3h^2}l^2\pi^2(h^2\pi^2a^2n^2 + h^2\pi^2b^2m^2 + 36a^2b^2),\\
C_{33} &= -\frac{12k_s\mu}{h^2} - \frac{1}{a^2b^2}\pi^2[(\lambda + 2\mu)a^2n^2 + \mu b^2m^2]\\
&\quad - \frac{\mu}{4a^4b^2h^2}l^2\pi^2[h^2\pi^2m^2(a^2n^2 + b^2m^2) + 12a^2(a^2n^2 + 4b^2m^2)],\\
C_{21} &= \frac{12}{h^2}C_{12},\quad C_{31} = \frac{12}{h^2}C_{13},\quad C_{32} = C_{23}.
\end{aligned} \tag{53}$$

Solving the linear algebraic equation system in Eq. (52) will yield W_{mn}, Φ^x_{mn} and Φ^y_{mn}. Then, substituting them into Eq. (48) will give the exact solutions w, ϕ_x, and ϕ_y based on the current non-classical model for the simply supported Mindlin plate subjected to the concentrated force at the center of the plate shown in Fig. 3.

The variations of the plate deflection w and rotation ϕ_x along the line $y = b/2$ predicted by the newly developed Mindlin plate model and by the classical Mindlin plate theory are plotted in Figs. 4 and 5, respectively. For illustration purposes, in the numerical analysis presented in this section, the plate is taken to be made of epoxy with the following properties: $E = 1.44$ GPa, $\nu = 0.38$, $l = 17.6\,\mu$m [1,18]. The shear correction factor k_s used is 0.8, which was shown to be the most accurate value for a homogeneous elastic Mindlin plate [34]. Also, the shape of the plate is fixed by letting $a = b = 20h$, while the plate thickness is varying.

In Figs. 4 and 5, the numerical results predicted by the current model are obtained from Eqs. (48), (52) and (53), while those by the classical model are computed using Eqs. (48), (52) and (53) with $l = 0$. The number of terms included in each of the three expansions in Eq. (48) is controlled by adjusting m and n. The numerical results obtained with $m = 20$ and $n = 20$ are found to be the same as those computed with larger m and n values (up to $m = 70$, $n = 70$) to the third decimal place for w, ϕ_x and ϕ_y, indicating that using $m = 20$, $n = 20$ in the expansions is sufficient for the convergent numerical solutions of w, ϕ_x and ϕ_y displayed in Figs. 4 and 5. Note that the values of ϕ_y along the line $x = a/2$ are the same as those of ϕ_x along

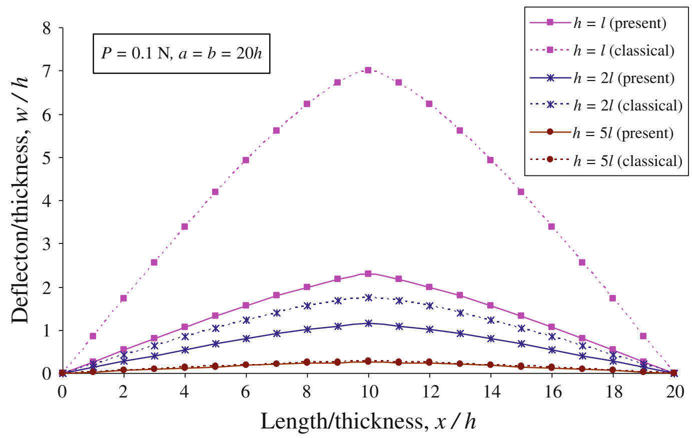

Fig. 4 Deflection of the simply supported Mindlin plate on $y = b/2$

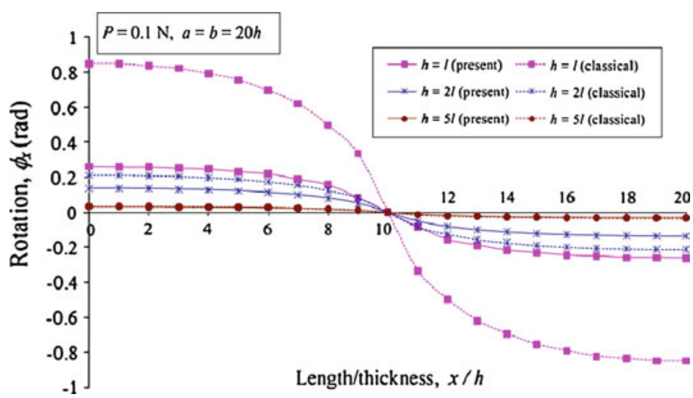

Fig. 5 Rotation of the simply supported Mindlin plate on $y = b/2$

the line $y = b/2$ due to the loading and geometrical symmetry of the square plate under consideration. Hence, ϕ_y is not plotted here.

It is clearly shown in Figs. 4 and 5 that both the deflection and rotation predicted by the current model are smaller than those predicted by the classical Mindlin plate model in all cases considered. It is also seen that the differences in the deflection and rotation values predicted by the current model and those predicted by the classical model are very large when the thickness of the plate, h, is small (with $h = l = 17.6\,\mu$m here), but they are diminishing as the thickness of the plate becomes large. This indicates that the size effect is only significant when the plate thickness is at the micron scale, which agrees with the general trends observed in experiments.

3.2 Free vibration

The free vibration of the simply supported plate shown in Fig. 3 is governed by Eqs. (36a–36e), with all external forces vanished (i.e., $f_x = 0,\ f_y = 0,\ f_z = 0,\ c_x = 0,\ c_y = 0,\ c_z = 0$), subject to the boundary conditions listed in Eqs. (44a–44c), (45a–45e), (46a–46c) and (47a–47e).

Since $f_x = f_y = 0$ and $c_z = 0$, Eqs. (36a, 36b), (44a), (45a, 45d), (46a) and (47a, 47d) give $u = u(x, y, t) \equiv 0,\ v = v(x, y, t) \equiv 0$ for any $(x, y) \in R$ and $t \in [0, T]$. For $w = w(x, y, t)$, $\phi_x = \phi_x(x, y, t)$, and $\phi_y = \phi_y(x, y, t)$, consider the following Fourier series expansions:

$$w(x, y, t) = \sum_{m=1}^{\infty}\sum_{n=1}^{\infty} W_{mn}^{V} \sin\left(\frac{m\pi x}{a}\right) \sin\left(\frac{n\pi y}{b}\right) e^{i\omega_n t},$$

$$\phi_x(x, y, t) = \sum_{m=1}^{\infty}\sum_{n=1}^{\infty} \Phi_{mn}^{x,V} \cos\left(\frac{m\pi x}{a}\right) \sin\left(\frac{n\pi y}{b}\right) \mathrm{e}^{i\omega_n t},$$
$$\phi_y(x, y, t) = \sum_{m=1}^{\infty}\sum_{n=1}^{\infty} \Phi_{mn}^{y,V} \sin\left(\frac{m\pi x}{a}\right) \cos\left(\frac{n\pi y}{b}\right) \mathrm{e}^{i\omega_n t}, \quad (54)$$

where ω_n is the nth natural frequency of vibration of the plate, W_{mn}^V, $\Phi_{mn}^{x,V}$ and $\Phi_{mn}^{y,V}$ are constant Fourier coefficients, and i is the usual imaginary number satisfying $i^2 = -1$. It can be shown that the expansions in Eq. (54) satisfy the boundary conditions in Eqs. (44b, 44c), (45b, 45c, 45e), (46b, 46c) and (47b, 47c, 47e).

Using Eq. (54) in Eqs. (36c–36e) yields

$$([C] + \rho\omega_n^2[I])[W_{mn}^V, \ \Phi_{mn}^{x,V}, \ \Phi_{mn}^{y,V}]^T = [0, \ 0, \ 0]^T, \quad (55)$$

where $[C]$ is the 3-by-3 matrix whose components are defined in Eq. (53), and $[I]$ is the 3-by-3 identity matrix. For an non-trivial solution of $W_{mn}^V \neq 0$, $\Phi_{mn}^{x,V} \neq 0$ and $\Phi_{mn}^{y,V} \neq 0$, it is required that the determinant of the coefficient matrix of Eq. (55) vanish. That is,

$$\left| \, [C] + \rho\omega_n^2[I] \, \right| = 0, \quad (56)$$

which can be expanded to obtain

$$\left(\rho\omega_n^2\right)^3 + I_C\left(\rho\omega_n^2\right)^2 + II_C\left(\rho\omega_n^2\right) + III_C = 0, \quad (57)$$

where

$$\begin{aligned} I_C &\equiv C_{ii} = C_{11} + C_{22} + C_{33}, \\ II_C &\equiv \frac{1}{2}\left(C_{ii}C_{jj} - C_{ij}C_{ji}\right) = C_{11}C_{22} + C_{22}C_{33} + C_{33}C_{11} - C_{12}C_{21} - C_{23}C_{32} - C_{13}C_{31}, \\ III_C &\equiv \varepsilon_{ijk}C_{i1}C_{j2}C_{k3} = C_{11}C_{22}C_{33} - C_{11}C_{23}C_{32} - C_{12}C_{21}C_{33} + C_{12}C_{23}C_{31} \\ &\quad + C_{13}C_{21}C_{32} - C_{13}C_{31}C_{22} \end{aligned} \quad (58)$$

are the three invariants of the $[C]$ matrix whose components C_{ij} are given in Eq. (53).

Equation (57) is a cubic equation in ω_n^2, the smallest (positive) root of which gives the nth natural frequency, ω_n, for the free vibration of the plate.

With ω_n determined from Eq. (57), W_{mn}^V, $\Phi_{mn}^{x,V}$ and $\Phi_{mn}^{y,V}$ (with two being independent) can then be obtained from solving Eq. (55), which will then lead to the determination of $w(x, y, t)$, $\phi_x(x, y, t)$ and $\phi_y(x, y, t)$ through Eq. (54), and thereby completing the solution.

Figure 6 displays the variation of the first natural frequency (with $m = 1$, $n = 1$ for the constants C_{ij} in Eq. (53)), ω_1, with the plate thickness predicted by the current model and by the classical Mindlin plate model. The results for the current non-classical Mindlin plate model shown in Fig. 6 are obtained from Eq. (57) along with Eqs. (58) and (53), while those for the classical Mindlin plate model are computed from Eqs. (57), (58), and (53) with $l = 0$. The material constants and geometry for the epoxy plate used here are the same as those employed earlier to obtain the numerical results displayed in Figs. 4 and 5. In addition, the density for the epoxy plate is taken to be $\rho = 1.22 \times 10^3$ kg/m^3 [37], which is needed to compute m_0 and m_2 from Eq. (22).

It is seen from Fig. 6 that the natural frequency predicted by the current model is always higher than that predicted by the classical model. Figure 6 also illustrates that the difference between the predictions by the current model and those by the classical plate model is significant only when the plate thickness is very small (with $h < 2l = 35.2\,\mu$m here). This shows that the size effect on the natural frequency is important only for very thin plates whose thickness is at the micron scale, which is a general trend observed in experiments.

It should be pointed out that the example problems of static bending and free vibration of a simply supported rectangular plate are analytically solved here for illustration purposes. Other problems involving a rectangular plate with different boundary conditions or a circular plate with various loading and support conditions may also be exactly solved by using the newly developed Mindlin plate model. However, such problems will need to be individually studied, considering that solutions for Mindlin plate problems tend to be long even in the context of classical elasticity (e.g., [38–41]).

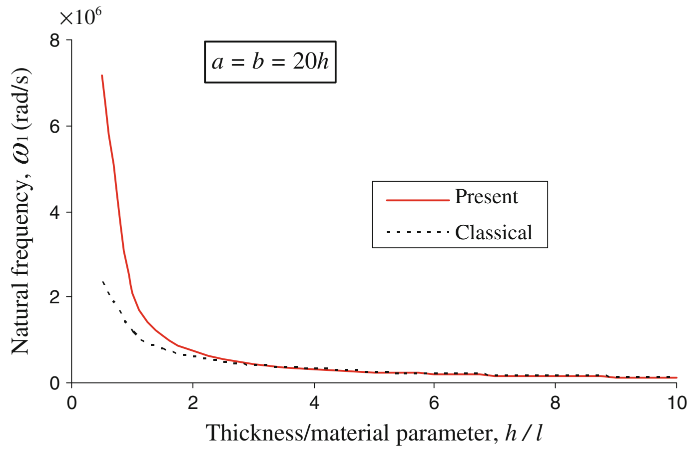

Fig. 6 Natural frequency varying with the plate thickness

4 Summary

A microstructure-dependent non-classical Mindlin plate model is developed using a modified couple stress theory. The equations of motion and boundary conditions for a Mindlin plate of arbitrary shape are obtained simultaneously via a variational formulation based on Hamilton's principle. The new model contains one material length scale parameter and can capture the size effect, unlike the classical Mindlin plate theory. Moreover, both bending and stretching deformations are considered, which differs from the classical Mindlin plate theory.

The current non-classical Mindlin plate model recovers the Timoshenko beam model based on the modified couple stress theory when the kinematic relations are specified to be those of the Timoshenko beam. Furthermore, the new Mindlin plate model developed here reduces to the classical Mindlin plate model when the material length scale parameter is set to be zero.

The static bending and free vibration problems of a simply supported plate are solved by directly applying the newly developed non-classical Mindlin plate model. The numerical results for the static bending problem reveal that both the deflection and rotations of the simply supported plate predicted by the new model are smaller than those predicted by the classical Mindlin plate model. Also, the differences in both the deflection and rotations predicted by the two models are very large when the plate thickness is small, but they are diminishing with the increase of the plate thickness. Similar trends are observed for the free vibration problem, where it is shown that the natural frequency predicted by the new model is higher than that by the classical model, with the difference between them being significantly large only for very thin plates. These predicted size effects in the plate bending at the micron scale agree with the general trend observed experimentally.

Acknowledgments The work reported in this paper is supported by a grant from the US National Science Foundation, with Dr. Clark V. Cooper as the program manager. This support is gratefully acknowledged. The authors also thank Professor George J. Weng and one anonymous reviewer for their encouragement and helpful comments on an earlier version of the paper.

References

1. Lam, D.C.C., Yang, F., Chong, A.C.M., Wang, J., Tong, P.: Experiments and theory in strain gradient elasticity. J. Mech. Phys. Solids **51**, 1477–1508 (2003)
2. McFarland, A.W., Colton, J.S.: Role of material microstructure in plate stiffness with relevance to microcantilever sensors. J. Micromech. Microeng. **15**, 1060–1067 (2005)
3. Lazopoulos, K.A.: On the gradient strain elasticity theory of plates. Euro. J. Mech. A Solids **23**, 843–852 (2004)
4. Altan, B.S., Aifantis, E.C.: On some aspects in the special theory of gradient elasticity. J. Mech. Behav. Mater. **8**(3), 231–282 (1997)
5. Gao, X.-L., Park, S.K.: Variational formulation of a simplified strain gradient elasticity theory and its application to a pressurized thick-walled cylinder problem. Int. J. Solids Struct. **44**, 7486–7499 (2007)
6. Gao, X.-L., Ma, H.M.: Solution of Eshelby's inclusion problem with a bounded domain and Eshelby's tensor for a spherical inclusion in a finite spherical matrix based on a simplified strain gradient elasticity theory. J. Mech. Phys. Solids **58**, 779–797 (2010)

7. Papargyri-Beskou, S., Beskos, D.E.: Static, stability and dynamic analysis of gradient elastic flexural Kirchhoff plates. Arch. Appl. Mech. **78**, 625–635 (2008)
8. Papargyri-Beskou, S., Giannakopoulos, A.E., Beskos, D.E.: Variational analysis of gradient elastic flexural plates under static loading. Int. J. Solids Struct. **47**, 2755–2766 (2010)
9. Eringen, A.C.: On differential equations of nonlocal elasticity and solutions of screw dislocation and surface waves. J. Appl. Phys. **54**, 4703–4710 (1983)
10. Lu, P., Zhang, P.Q., Lee, H.P., Wang, C.M., Reddy, J.N.: Non-local elastic plate theories. Proc. R. Soc. A **463**, 3225–3240 (2007)
11. Tsiatas, G.C.: A new Kirchhoff plate model based on a modified couple stress theory. Int. J. Solids Struct. **46**, 2757–2764 (2009)
12. Jomehzadeh, E., Noori, H.R., Saidi, A.R.: The size-dependent vibration analysis of micro-plates based on a modified couple stress theory. Phys. E **43**, 877–883 (2011)
13. Yang, F., Chong, A.C.M., Lam, D.C.C., Tong, P.: Couple stress based strain gradient theory for elasticity. Int. J. Solids Struct. **39**, 2731–2743 (2002)
14. Park, S.K., Gao, X.-L.: Variational formulation of a modified couple stress theory and its application to a simple shear problem. Z. Angew. Math. Phys. **59**, 904–917 (2008)
15. Lazopoulos, K.A.: On bending of strain gradient elastic micro-plates. Mech. Res. Commun. **36**, 777–783 (2009)
16. Li, S.: On the micromechanics theory of Reissner–Mindlin plates. Acta Mech. **142**, 47–99 (2000)
17. Li, S.: The micromechanics theory of classical plates: a congruous estimate of overall elastic stiffness. Int. J. Solids Struct. **37**, 5599–5628 (2000)
18. Park, S.K., Gao, X.-L.: Bernoulli–Euler beam model based on a modified couple stress theory. J. Micromech. Microeng. **16**, 2355–2359 (2006)
19. Ma, H.M., Gao, X.-L., Reddy, J.N.: A microstructure-dependent Timoshenko beam model based on a modified couple stress theory. J. Mech. Phys. Solids **56**, 3379–3391 (2008)
20. Ma, H.M., Gao, X.-L., Reddy, J.N.: A non-classical Reddy–Levinson beam model based on a modified couple stress theory. Int. J. Multiscale Comput. Eng. **8**, 167–180 (2010)
21. Mindlin, R.D.: Influence of couple-stresses on stress concentrations. Exp. Mech. **3**, 1–7 (1963)
22. Mindlin, R.D., Tiersten, H.F.: Effects of couple-stresses in linear elasticity. Arch. Ration. Mech. Anal. **11**, 415–448 (1962)
23. Koiter, W.T.: Couple-stresses in the theory of elasticity. Proc. K. Ned. Akad. Wet. B **67**, 17–44 (1964)
24. Timoshenko, S.P., Goodier, J.N.: Theory of Elasticity, 3rd edn. McGraw-Hill, New York (1970)
25. Horgan, C.O.: On the strain-energy density in linear elasticity. J. Eng. Math. **7**, 231–234 (1973)
26. Fung, Y.C., Tong, P.: Classical and Computational Solid Mechanics. World Scientific, Singapore (2001)
27. Chong, A.C.M., Yang, F., Lam, D.C.C., Tong, P.: Torsion and bending of micron-scaled structures. J. Mater. Res. **16**, 1052–1058 (2001)
28. Nikolov, S., Han, C.-S., Raabe, D.: On the origin of size effects in small-strain elasticity of solid polymers. Int. J. Solids Struct. **44**, 1582–1592 (2007)
29. Reddy, J.N.: Energy Principles and Variational Methods in Applied Mechanics, 2nd edn. Wiley, New York (2002)
30. Reddy, J.N.: Theory and Analysis of Elastic Plates and Shells, 2nd edn. Taylor & Francis, Philadelphia (2007)
31. Gao, X.-L., Mall, S.: Variational solution for a cracked mosaic model of woven fabric composites. Int. J. Solids Struct. **38**, 855–874 (2001)
32. Stephen, N.G.: Mindlin plate theory: best shear coefficient and higher spectra validity. J. Sound Vib. **202**, 539–553 (1997)
33. Wang, C.M., Lim, G.T., Reddy, J.N., Lee, K.H.: Relationships between bending solutions of Reissner and Mindlin plate theories. Eng. Struct. **23**, 838–849 (2001)
34. Liu, Y., Soh, C.-K.: Shear correction for Mindlin type plate and shell elements. Int. J. Numer. Meth. Eng. **69**, 2789–2806 (2007)
35. Batista, M.: An elementary derivation of basic equations of the Reissner and Mindlin plate theories. Eng. Struct. **32**, 906–909 (2010)
36. Mindlin, R.D.: Influence of rotatory inertia and shear on flexural motions of isotropic, elastic plates. ASME J. Appl. Mech. **18**, 1031–1036 (1951)
37. Maneschy, C.E., Miyano, Y., Shimbo, M., Woo, T.C.: Residual-stress analysis of an epoxy plate subjected to rapid cooling on both surfaces. Exp. Mech. **26**, 306–312 (1986)
38. Cooke, D.W., Levinson, M.: Thick rectangular plates–II: the generalized Lévy solution. Int. J. Mech. Sci. **25**, 207–215 (1983)
39. Kabir, H.R.H., Chaudhuri, R.A.: Boundary-continuous Fourier solution for clamped Mindlin plates. ASCE J. Eng. Mech. **118**, 1457–1467 (1992)
40. Naumenko, K., Altenbach, J., Altenbach, H., Naumenko, V.K.: Closed and approximate analytical solutions for rectangular Mindlin plates. Acta Mech. **147**, 153–172 (2001)
41. Batista, M.: Refined Mindlin–Reissner theory of forced vibrations of shear deformable plates. Eng. Struct. **33**, 265–272 (2011)